ELSEVIER

Polymer 42 (2001) 3527–3632

polymer

www.elsevier.nl/locate/polymer

Investigation of the stiffness change in, the indentation force and the hydrophobic recovery of plasma-oxidized polydimethylsiloxane surfaces by tapping mode atomic force microscopy

G. Bar[a,1,*], L. Delineau[a], A. Häfele[a], M.-H. Whangbo[b]

[a]*Freiburger Materialforschungszentrum and Institut für Makromolekulare Chemie, Albert-Ludwigs Universität, Stefan Meier-Str. 21, 79104 Freiburg, Germany*

[b]*Department of Chemistry, North Carolina State University, Raleigh, NC, 27695-8204, USA*

Received 18 July 2000; received in revised form 25 August 2000; accepted 25 September 2000

Abstract

Polydimethylsiloxane (PDMS) samples of different crosslink densities were oxidized in air plasma, and the stiffness change in the oxidized PDMS surface was monitored by performing tapping mode atomic force microscopy (TMAFM) distance-sweep measurements and numerical simulations of the cantilever equation of motion based on a contact mechanics model. The diffusion mechanism of hydrophobic recovery of an oxidized PDMS surface was examined by a combined use of TMAFM distance-sweep and phase imaging experiments. Our work shows that the modulus of the oxidized PDMS surface increases with increasing the oxidation time, and supports the diffusion mechanism of hydrophobic recovery. It is possible to extract information about the indentation force from observed indentation curves and to employ TMAFM for force modulation experiments at high modulation frequency.

Keywords: Polydimethylsiloxane; Tapping mode atomic force microscopy; X-ray photoelectron spectroscopy

1. Introduction

Among physical and chemical modifications of polymer surfaces corona and plasma treatments of polymers are of practical importance for many applications. For example, in biomedical applications such as contact lenses and blood-contacting devices, a wettable surface is desired [1]. Polydimethylsiloxane (PDMS) has a hydrophobic surface, and oxygen plasma or corona treatments can be used to make its surface hydrophilic and improve its wettability (needed for biomedical applications) [2]. From fundamental and practical viewpoints, it is therefore crucial to understand what physical and chemical changes corona or plasma treatments bring about. It is known that the hydrophilicity of PDMS surfaces induced by corona and plasma treatments is lost with time, which is referred to as hydrophobic recovery [3]. This phenomenon has been the subject of many studies and several explanations have been put forward for the mechanism of hydrophobic recovery [3–6]. A number of experimental methods such as contact angle measurements, Fourier transform infrared (FTIR) reflectance, X-ray photoelectron spectroscopy (XPS) and static secondary ion mass spectroscopy (SSIMS) have been used to characterize the wettability of and the chemical changes in plasma-oxidized PDMS surfaces. However, very little is known about the local mechanical changes caused by the plasma treatment, and the structures of plasma-treated surfaces are not completely understood. Nevertheless, the plasma oxidation is believed to introduce new crosslinks through the formation of new Si–O–Si bonds because FTIR, XPS and SSIMS data indicate that the oxidation converts the sample surface into a silica (SiO_2)-like layer with thickness ranging from several tens to several hundreds of nanometers depending on oxidation time and intensity [3,7]. It has been suggested that cracks are formed on the brittle silica-like surface due to mechanically and/or thermally induced stresses, and these cracks allow unoxidized low molecular weight PDMS lying under the oxidized surface to ooze out covering the surface and hence causing hydrophobic recovery [3] (hereafter referred to as the diffusion mechanism of hydrophobic recovery). Recently Bowden et al. [8] showed that complex patterns form spontaneously when PDMS is first heated, then

* Corresponding author. Tel.: +31-115-67-2302; fax: +31-115-67-3729.
E-mail address: gkbar@dow.com (G. Bar).
[1] Current address: Dow Benelux N.V. Analytical Sciences, PO Box 48, 4530 AA Terneuzen, The Netherlands.

0032-3861/01/$ - see front matter
PII: S0032-3861(00)00738-2

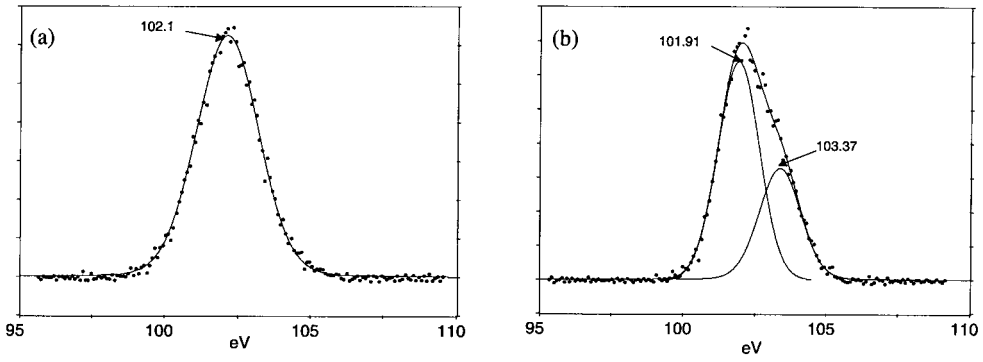

Fig. 1. Si 2p peaks of the XPS spectra obtained for unoxidized and oxidized PDMS samples: (a) unoxidized "1.2" sample; (b) "1.2" sample exposed to air plasma for 30 s.

exposed to oxygen plasma and finally cooled. To explain this observation they had to assume that the plasma oxidation increases the modulus of the surface. This assumption is quite reasonable given that the surface of PDMS is converted to a brittle, silica-like layer under oxidation. Nevertheless, it is important to monitor directly the mechanical changes induced by the plasma oxidation and provide direct experimental evidence for supporting this assumption.

In the present study we employ tapping mode atomic force microscopy (TMAFM) [9] to monitor stiffness changes in plasma-treated PDMS surfaces and provide support for the diffusion mechanism of hydrophobic recovery. In recent years TMAFM [10] is routinely used to study structures, morphologies and compositions of various polymer surfaces because it provides enhanced image contrasts and resolution [11]. Phase images of TMAFM depend sensitively on local materials properties and also on experimental parameters (e.g. the free amplitude A_0, the set-point amplitude A_{sp}, the tip shape, and the force constant k_0 of a free cantilever) [12]. The repulsive tip–sample force interactions are often described by the Hertzian contact mechanics model [13], in which the indentation force of a tip–sample system in static contact is related to the indentation depth. To gain insight into the tip–force interaction, TMAFM experiments are carried out in frequency- or distance-sweep mode. When the amplitude and phase angle are recorded as a function of the tip–sample rest distance z at a fixed drive frequency, one obtains $A(z)$ and $\Phi(z)$ curves. These curves can be simulated by numerically solving the equation of motion for a tapping cantilever within the framework of an appropriate contact mechanics model. Recent experimental and numerical simulation studies have shown [14–16] that a cantilever tapping on compliant samples deeply indents their surfaces and behaves like a simple harmonic oscillator. In the present work we monitor the stiffness change in plasma-oxidized PDMS surfaces by performing distance-sweep (Z-sweep) TMAFM experiments as well as numerical simulations of the resulting $A(z)$ curves.

2. Experimental

The PDMS samples used in our study are very compliant elastomers. They were prepared by mixing a base and a cure agent in the 15:x ratio (e.g. $x = 0.6$, 0.9, 1.2) by weight and then heating to induce a crosslink reaction. The crosslink density, and hence the elastic modulus, of a PDMS sample increases with increasing the x value. Our dynamic mechanical analysis (DMA) [17] shows that the unoxidized PDMS samples with $x = 0.6$, 0.9 and 1.2 (hereafter referred to as "0.6", "0.9" and "1.2" samples) have storage moduli of 0.50, 0.97 and 1.32 MPa, respectively, at room temperature. The DMA data show a typical rubber-like behavior. All the unoxidized samples have very similar glass transition temperature ($T_g \approx -119°C$), density ($\rho \approx 1.02$ g/cm^3) and surface free energy (advancing contact angle $\theta \approx 110°$). The PDMS samples were exposed to air plasma in a home-built apparatus for 1 s to 30 min using a power of 1.5 W and a pressure of about 0.1 mbar.

XPS measurements were carried out for oxidized and unoxidized PDMS samples to confirm the oxidized nature of the plasma-treated PDMS surfaces. As shown in Fig. 1a, the Si 2p peak of an unoxidized PDMS sample, located at 102.1 eV, is symmetrical. Fig. 1b shows that the Si 2p peak of the plasma-treated PDMS for 30 s is unsymmetrical, and is decomposed into two peaks located at 109.1 and 103.4 eV. As the oxidation time increases, the lower-energy peak diminishes while the higher-energy peak grows. These features are identical with those reported by Hillborg and Gedde [3], and indicate that oxidation on PDMS surfaces involves the formation of linkages between Si and O atoms.

The TMAFM measurements were performed using a Nanoscope III scanning probe microscope immediately after the treatment as well as after several hours to monitor the effect of aging. We used commercial Si cantilevers with spring constants $k_0 = 34$ N/m and resonance frequencies $\omega_0 = 2\pi \times 166$ kHz. All TMAFM measurements were carried out at ambient conditions and by driving the cantilever at its resonance frequency. The Z-sweep experiments were performed with free amplitude $A_0 \approx 73$ nm. In this

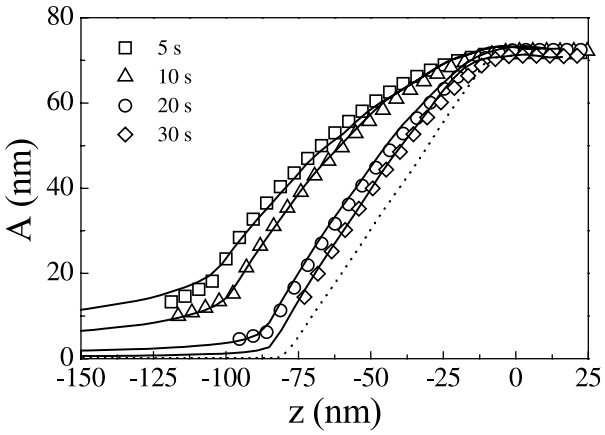

Fig. 2. Experimental (open symbols) and simulated (solid lines) amplitude curves as a function of z for the "1.2" sample. The squares, triangles, circles and diamonds refer to the samples exposed to plasma for 5, 10, 20 and 30 s, respectively. The tip–sample reduced moduli E^* used to simulate the experimental $A(z)$ curves for the samples for 5, 10, 20 and 30 s plasma oxidation are 14, 25, 80 and 220 MPa, respectively. The dotted line represents the $A(z)$ curve simulated for a very stiff surface (with $E^* = 100$ GPa).

Z-sweep method, the lateral position of the tip is fixed, and the amplitude and phase angle of a tapping cantilever are measured as a function of the tip–sample rest distance z. Z-sweep measurements lead to amplitude vs. distance and phase vs. distance curves, i.e. $A(z)$ and $\Phi(z)$ curves, respectively [14,16].

3. Stiffness change and indentation force

3.1. Effect of oxidation on amplitude

For the "1.2" samples exposed to air plasma for 5, 10, 20 and 30 s, the amplitude $A(z)$ is plotted as a function of z in Fig. 2. The samples oxidized for 5 s have the $A(z)$ curves very similar to those found for the unoxidized samples. The $A(z)$ curves exhibit a nonlinear decrease with decreasing z. As z begins to decrease, the amplitude decreases slowly compared with the case of stiff materials. As described earlier [14,16], this stems from the fact that the tip deeply indents sample surfaces (see below). With decreasing z further, the $A(z)$ curves decrease steadily until a certain large negative z value, below which the $A(z)$ curves decrease very slowly. As the oxidation time is increased, the $A(z)$ curves decrease faster with decreasing z, the sharp decrease in the slope of $A(z)$ occurs at a smaller negative z, and the amplitude approaches a smaller value in the region of large negative z. When the oxidation time exceeds 30 s, the $A(z)$ curves decrease almost linearly with decreasing z, and their shape does not alter significantly with further increasing the oxidation time. (Though not shown, similar results are obtained for the "0.6" and "0.9" samples. Thus we will present results obtained only for the "1.2" samples.)

The solid lines in Fig. 2 show the $A(z)$ curves obtained by numerical simulations using a commercially available software package [18]. For our simulation study, the Burnham, Colton and Pollock [19] contact mechanics model was selected. The parameters used are the force constant $k_0 = 34$ N/m, the resonance frequency $\omega_0 = 2\pi \times 166$ kHz and the quality factor $Q_0 = 400$ of a free cantilever as well as the drive frequency $\omega = \omega_0$ and the tip–sample reduced radius of curvature $R = 10$ nm. These parameters are based on experimental values. The ratio of the tip–sample interaction damping to the viscous damping in air (i.e. γ_i/γ_v) was chosen between 1 and 2, because our experimental studies showed that the quality factor of a tapping cantilever decreases from that of a free cantilever by about 2 when the tip–sample interaction is increased [13]. According to our DMA study [17], the elastic storage moduli of unoxidized PDMS samples are in the range of 8 MPa at 100 kHz. The latter means that the tip–sample reduced modulus E^* is about 14 MPa since a silicon tip was employed in our study. The dotted line of Fig. 2 represents the amplitude curve calculated (using $E^* = 100$ GPa) for very stiff samples (e.g. Si and SiO_2) on which the indentation δ is practically zero, and will be referred to as the $A_{st}(z)$ curve.

The experimental $A(z)$ curves are reproduced by numerical simulation when the reduced modulus E^* of an oxidized PDMS is assumed to increase with increasing the oxidation time. The $A(z)$ curves recorded for the PDMS samples

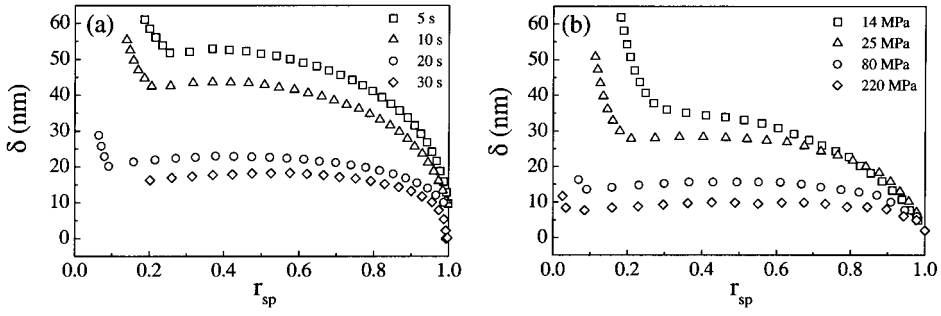

Fig. 3. (a) Experimental and (b) simulated indentation depths $\delta(r_{sp})$ of for the "1.2" samples as a function of r_{sp}. In (a) the squares, triangles, circles and diamonds refer to the samples exposed to plasma for 5, 10, 20 and 30 s, respectively. In (b) the squares, triangles, circles and diamonds refer to the results of simulation obtained with $E^* = 14$, 25, 80 and 220 MPa, respectively.

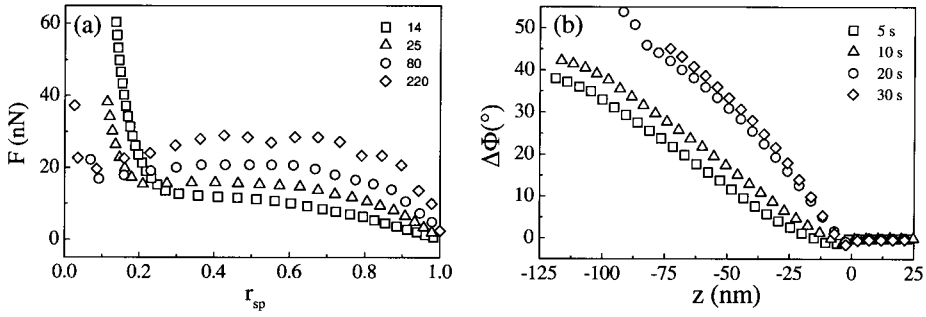

Fig. 4. (a) Indentation force curves $F(r_{sp})$ associated with the $\delta(r_{sp})$ curves calculated for the "1.2" samples. The squares, triangles, circles and diamonds refer to the $F(r_{sp})$ curves for $E^* = 14$, 25, 80 and 220 MPa, respectively. (b) Phase shifts $\Delta\Phi$ recorded for the "1.2" samples as a function of z. The squares, triangles, circles and diamonds refer to the samples exposed to plasma for 5, 10, 20 and 30 s, respectively.

exposed to air plasma for 5, 10, 20 and 30 s are well reproduced by using $E^* = 14$, 25, 80 and 220 MPa, respectively. The $A(z)$ curves of the oxidized PDMS samples lie above the $A_{st}(z)$ curve due to the indentation on these samples. With increasing the oxidation time, the resulting $A(z)$ curve becomes more similar to the $A_{st}(z)$ curve because the indentation decreases. The agreement between the experimental and simulated $A(z)$ curves is quite excellent, although there is some uncertainty in the tip shape and radius as well as in the validity of the chosen contact mechanics model for highly viscoelastic materials.

3.2. Effect of oxidation on indentation

The tip indentation δ on a compliant sample can be determined as a function of z and as a function of the set-point ratio $r_{sp} = A/A_0$ from the experimental $A(z)$ curves [16]. The $A(z)$ curves observed for the oxidized PDMS samples lie above the $A_{st}(z)$ curve (Fig. 2). For a stiff sample the indentation is essentially zero, so that the $A_{st}(z)$ curve is given by $A_{st}(z) = A_0 - |z|$. The deformation of the stiff silicon tip is negligible compared with that of the PDMS samples. Thus, for a given PDMS sample, the indentation depth $\delta(z)$ at a given z is practically given by $\delta(z) = A(z) - A_{st}(z)$[16]. The $\delta(r_{sp})$ curves derived from the $\delta(z)$ curves for the "1.2" sample are presented in Fig. 3a. At a given r_{sp}, the indentation δ decreases by more than a factor of two as the oxidation time is increased from 5 to 30 s. With decreasing r_{sp}, the $\delta(r_{sp})$ curves for short oxidation time first increase fast, saturate at moderate r_{sp} values, and then increase sharply below a certain small r_{sp} value. The sharp increase in $\delta(r_{sp})$ at small r_{sp} corresponds to the sharp decrease in the slope of the corresponding $A(z)$ curves at large negative z (Fig. 2). Fig. 3b shows the calculated $\delta(r_{sp})$ curves determined from the calculated $A(z)$ curves. As expected from the good agreement between the experimental and simulated $A(z)$ curves in Fig. 2, the calculated $\delta(r_{sp})$ curves are quite close to the experimental $\delta(r_{sp})$ curves.

3.3. Indentation force and phase shift

To understand the cause for the sharp increase in the $\delta(r_{sp})$ curves at low r_{sp} and its implications, we examine the calculated indentation force curves $F(r_{sp})$, shown in Fig. 4a, which are associated with the calculated $\delta(r_{sp})$ curves of Fig. 3b. It is clear from Figs. 3b and 4a that the

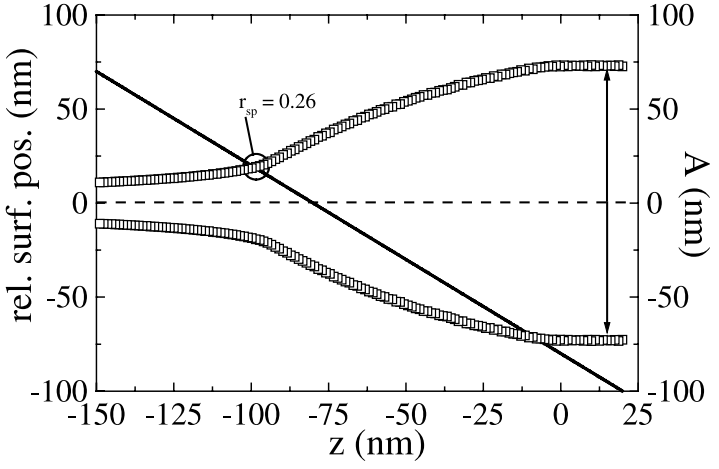

Fig. 5. Upper and lower turning points of oscillation (squares) calculated for the "1.2" sample with $E^* = 14$ as a function of the tip–sample rest distance z. The solid line refers to the relative position of the surface as a function of z, and the dashed line to the rest position of the tip.

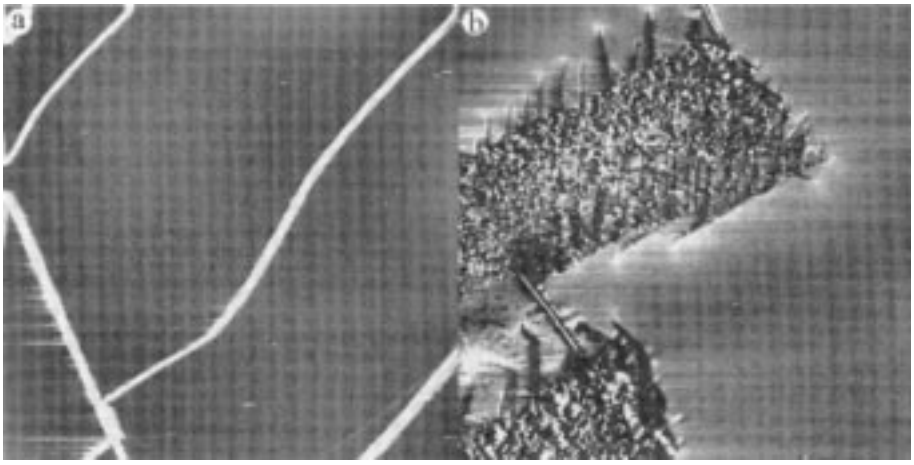

Fig. 6. Phase images of the "1.2" sample treated with plasma for 5 min after heating at 150°C for 1 h 30 min. The scan size is 90 μm in (a), and 25 μm in (b).

r_{sp}-dependences of the $F(r_{sp})$ curves are quite similar to those of the $\delta(r_{sp})$ curves. This is not surprising because in the Hertzian contact mechanics the indentation force is related to the indentation depth by $F \propto \delta^{1.5}$ (for a spherical body in contact with a flat surface) [13]. Nevertheless, it is important to recognize from the above result and the closeness of the experimental and calculated $\delta(r_{sp})$ curves that information about the indentation force can be gained from the experimental $\delta(r_{sp})$ curves. Fig. 4a shows that the indentation force $F(r_{sp})$ increases with increasing the sample modulus in the region of $0.2 < r_{sp} < 1$.

The phase angles $\Phi(z)$ recorded for the "1.2" samples are plotted as a function of the tip–sample rest distance z in Fig. 4b. The $\Phi(z)$ curves for the sample with 5 s oxidation are very similar to those for unoxidized samples, as expected from the corresponding $A(z)$ curves. For a given z, a longer oxidation time leads to a greater positive phase shift. This result is expected, because the phase shift $\Delta\Phi$ is governed by two factors, i.e. the frequency shift $\Delta\omega$ and the effective quality factor Q_{eff}. For compliant elastomers the Q_{eff} term is related to the viscous damping and the energy dissipation caused by tip–sample interaction. The $\Delta\omega$ term is related to the force constant change Δk in the tapping cantilever, namely, $\Delta\omega = \Delta k(\omega_0/2k_0)$, and therefore to the tip–sample reduced modulus (in the repulsive tip–sample interaction regime) [13,20,21]. Thus the phase curves also indicate that the reduced modulus of the oxidized PDMS surface increases with increasing the oxidation time.

4. Quasi force modulation with TMAFM

We now probe the cause for the sharp decrease in the slopes of the $A(z)$ curves at large negative z (equivalently, the sharp increase in the $\delta(r_{sp})$ curves at small r_{sp}) by studying the cantilever amplitude calculated during numerical simulations. Fig. 5 presents the highest and lowest positions of the oscillating tip (i.e. the upper and lower turning points of the cantilever oscillation, respectively) calculated for the case of $E^* = 14$ MPa (squares) as a function of z. The relative surface position (solid line) is also shown as a function of z. Here the zero of the relative surface position (dashed line) is equal to the rest position of the tip. The tip does not touch the surface when the lower turning point lies above the solid line, but it does otherwise. When the upper turning point lies above the solid line, the tip is in intermittent contact with the surface during each cycle of oscillation so that the cantilever taps the surface. However, in the region of z where the upper turning point lies below the solid line, the tip is in permanent contact with the surface during each cycle of oscillation so that the function of an oscillating cantilever becomes quasi force modulation [22] instead of tapping.

Thus the sharp decrease in the slopes of the $A(z)$ curves at large negative z (Fig. 2) and the sharp increase in the $\delta(r_{sp})$ curves at small r_{sp} (Fig. 3a) signify that the oscillating cantilever switches its role from tapping to force modulation. This suggests that TMAFM can be used for force modulation experiments. Since the drive frequency of the cantilever is typically high (e.g. 100–300 kHz range) in TMAFM, such experiments might allow one to extract information about the storage and loss moduli of elastomers at high modulation frequencies. This question will be probed in detail elsewhere [17].

5. Hydrophobic recovery

In this section we discuss the diffusion mechanism of hydrophobic recovery by studying the effect of mechanical stress on the oxidized surface of PDMS. For this purpose the "1.2" samples were heated at 150°C for 1 h 30 min and then immediately exposed to air plasma for 30 s to 30 min. Fig. 6a and b show TMAFM phase images for such thermally treated "1.2" samples exposed to plasma for 5 min. Cracks up to several tens of microns (Fig. 6a) and a significant change in surface roughness at higher magnifications (Fig. 6b) are observed. Thermal treatment leads to an expansion

of the PDMS sample and upon cooling the sample shrinks causing a mechanical stress due to the silica-like thin film on the surface. Shorter time of oxidation or heating results in less and smaller cracks. For thermally untreated samples exposed to plasma for a short time (up to 30 s), cracks were generally not observed although the presence of some local cracks and increased roughness cannot be excluded. As expected, we observed hydrophobic recovery for the plasma-oxidized PDMS samples. However, even after leaving such samples in ambient conditions for hours or days, we found that the $A(z)$ curves determined after hydrophobic recovery are practically identical with those determined before hydrophobic recovery. Therefore our results support the diffusion mechanism of hydrophobic recovery.

6. Concluding remarks

Our work shows that the modulus of the oxidized PDMS surface increases with increasing the oxidation time, that information about the indentation force can be extracted from the observed indentation curves, and that hydrophobic recovery occurs most likely by the diffusion mechanism. On compliant polymers the function of an oscillating cantilever can switch from tapping to force modulation. The latter suggests the possibility of using TMAFM for force modulation experiments at high modulation frequencies.

Acknowledgements

G. Bar wishes to thank the Deutsche Forschungsgemeinschaft for the financial support under Grant BA 1285/4-1. Work at North Carolina State University was supported by the Office of Basic Energy Sciences, Division of Materials Sciences, US Department of Energy, under Grant DE-FG05-86ER45259.

References

[1] Fakes DW, Davies MC, Brown A, Newton JM. Surf Interface Anal 1988;13:233.
[2] Garbassi F, Morra M, Occhiello E. Polymer surfaces: from physics to technology. Chichester, UK: Wiley, 1998.
[3] Hillborg H, Gedde UW. Polymer 1991;39:484.
[4] Lee CL, Homan GR. Annual Report No. 81CH1668-3, Conference on Electrical Insulating and Dieelectric Phenomenon IEEE Electrical Insulating Society, 1981.
[5] Owen MJ, Gentle TM, Orbeck T, Williams DE. In: Andrade JD, editor. Polymer surface dynamics. New York: Plenum, 1988.
[6] Morra M, Occhiello E, Marola R, Garbassi F, Humphrey P, Johnson D. J Colloid Interface Sci 1990;137:11.
[7] Toth A, Bertoti I, Blazso M, Banhegyi G, Bognar A, Szaplonczay X. J Appl Polym Sci 1994;39:265.
[8] Bowden N, Huck WTS, Paul KE, Whitsides GM. Appl Phys Lett 1995;75:2557.
[9] Zhong Q, Innis D, Kjoller K, Elings VB. Surf Sci Lett 1993;290:L688.
[10] Chernoff DA. Proceedings microscopy and microanalysis. New York: Jones and Begell, 1995.
[11] Magonov SN, Reneker DH. Annu Rev Mater Sci 1997;27:175.
[12] Bar G, Thomann Y, Brandsch R, Cantow H-J, Whangbo M-H. Langmuir 1997;13:3807.
[13] Hertz H, Reine J. Angew Math 1888;92:156.
[14] Delineau L, Brandsch R, Bar G, Whangbo M-H. Surf Sci Lett 2000;448:L179.
[15] Behrend OP, Odonii L, Loubet JL, Burnham NA. Appl Phys Lett 1995;75:2551.
[16] Bar G, Delineau L, Brandsch R, Bruch M, Whangbo M-H. Appl Phys Lett 1995;75:4198.
[17] Bar G, Delineau L, Whangbo M-H. In preparation.
[18] Nanomechanics LLC, http://www.nanomechanics.com.
[19] Burnham NA, Kulik AJ. In: Bhushan B, editor. Handbook of micro/nanotribology, 2nd ed. Boca Raton, FL: CRC Press, 1999.
[20] Bar G, Brandsch R, Bruch M, Delineau L, Whangbo M-H. Surf Sci Lett 2000;444:L11.
[21] Magonov SN, Elings V, Whangbo M-H. Surf Sci Lett 1997;375:L385.
[22] Maivald P, Butt H-J, Gould SAC, Prater CB, Drake B, Gurley JA, Elings VB, Hansma PK. Nanotechnology 1991;2:103.